ME-87-02

Chloride Corrosion Threshold in Concrete

Ontario
Ministry of Transportation and Communications

Research and Development Branch

ME-87-02

Chloride Corrosion Threshold in Concrete

B.B. Hope
A.K.C. Ip

Queen's University, Kingston

Published by
The Research and Development Branch
Ontario Ministry of Transportation and Communications
Hon. Ed Fulton, Minister
D.G. Hobbs, Deputy Minister

Published without prejudice as to the application of the findings. Crown copyright reserved; however, this document may be reproduced for non-commercial purposes with attribution to the Ministry.

For additional copies, write:
The Editor, Technical Publications
Room 320, Central Building
1201 Wilson Avenue
Downsview, Ontario
Canada M3M 1J8

Telephone: (416) 235-7635
Infotex Electronic Mail: 23:MIN006

March 1987

Technical Report Documentation Page

Chloride Corrosion Threshold in Concrete

Author:	B.B. Hope, A.K.C. Ip
MTC No.:	ME-87-02
Date:	March 1987
Published by:	The Research and Development Branch Ontario Ministry of Transportation and Communications
MTC Contact:	Hannah Schell
Abstract:	The effects of chloride in concrete containing admixed calcium chloride dihydrate and chloride bearing aggregates on microcell and macrocell corrosion were studied. Test specimens were concrete slabs containing either single steel rods or electrically connected steel and subjected to various outdoor and indoor exposure conditions. Corrosion of the single rods was examined by the linear polarization and gravimetric mass loss method. Corrosion of the electrically coupled steel was monitored by measurement of the current flows between the anode and cathode steel and by visual inspection. The pH and chloride measurements for the concretes were conducted at the end of the test period. Corrosion rates of the single steel increased with increasing chloride content. The chloride corrosion threshold limit was between about 0.2% and 0.4% calcium chloride dihydrate by mass of cement (0.014% and 0.022% soluble chloride ion by mass of concrete) depending on the test method. Macrocell corrosion rate with electrically coupled steel was influenced greatly by the differential concentration of chloride ions in anode and cathode regions; large differences in chloride concentration resulted in a high corrosion rate. Chloride in the chloride-bearing aggregates used for this investigation appeared not to be available, to any significant degree for the corrosion process. The pH of the concretes were in the range from about 12 to 12.5, regardless of the chloride content and aggregate type.
Comments:	Final Report of Research and Development Branch Project No. 22134 conducted under the Ontario Joint Transportation and Communications Research Program
Key words:	corrosion of steel in concrete, chloride, chloride-bearing aggregates, corrosion rate measurement, corrosion threshold
Distribution:	MTC Districts and Regions, other highway agencies and corrosion researchers
Copyright Status:	Crown copyright

Table of Contents

1/ Introduction	1
2/ Experimental Work	2
2.1/ Specimens	2
2.2/ Storage and Test Schedule	3
2.3/ Concrete Resistivity Measurement	4
2.4/ Corrosion Measurement	5
3/ Results	5
4/ Discussion	7
4.1/ Measured Chloride Contents	7
4.2/ Microcell Specimens	7
4.3/ Macrocell Specimens	10
4.4/ Alkalinity	11
5/ Conclusions	11
References	12

List of Tables

1/ Microcell Slabs 14

2/ Macrocell Slabs 14

3/ Chemical Analysis of the Portland Cement 15

4/ Mix Design for the Concrete 15

5/ Concrete Resistivities for the Indoor Microcell Slabs 16

6/ Steel Potentials for the Indoor Microcell Slabs 17

7/ Corrosion Currents in the Indoor Microcell Slabs 18

8/ Electrochemical and Gravimetric Mass Loss of Typical Rods in the Microcell Slabs Subjected to the Oven-Dried Cycle 19

9/ Measured Chloride Contents of the Concrete 20

List of Figures

1/ Microcell Slab 21

2/ Microcell Slab 1 21

3/ Microcell Slab 2 22

4/ Outdoor Storage 22

5a/ Indoor Storage – Air Drying Period 23

5b/ Indoor Storage – Water Soaking Period 23

6/ Corrosion Currents, Steel Potentials, and Concrete Resistivities for the 0.8% Admixed Chloride Microcell Slabs Stored Outdoors and Subjected to the 3 Day/11 Day Wet/Dry Cycle 24

7/ Corrosion Currents, Steel Potentials, and Concrete Resistivities for the 0.8% Admixed Chloride Microcell Slabs Subjected to the Oven-Dried Cycle 24

8/ Average Corrosion Currents in the Admixed Chloride Microcell Slabs Subjected to the Oven-Dried Cycle 25

9/ Impedance Diagram for the Steel in a 2% Admixed Chloride Microcell Slab 25

10/ Impedance Diagram for the Steel in a Chloride-Aggregate Microcell Slab 26

11/ Impedance Diagram for the Steel in a Chloride-Aggregate Microcell Slab at High Frequencies 26

12/ Corrosion on the Steel Embedded in the Outdoor Microcell Slabs 27

13/ Corrosion of Steel Embedded in the Microcell Slabs Subjected to the Oven-Dried Cycle 27

14/ Corrosion Currents in the Indoor Macrocell Slabs 28

15/ Corrosion Currents, Anode/Cathode Potential Differences and Concrete Resistivities for the 2% Chloride to Chloride-Free Macrocell Slabs 28

16/ Corrosion on the Anode Steel Embedded in the Outdoor Macrocell Slabs 29

17/ Measured Chloride Content of the Admixtured Chloride Concrete 29

NOTATION

R_c = concrete electrical resistance, ohms

R_e = electrolyte resistance, ohms

R_t = charge transfer resistance, ohms

R_f = passive film resistance, ohms

R_p = polarization resistance, ohms

ρ_c = concrete electrical resistivity, ohm-cm

E_o = corrosion potential, - mV CSE

δE = instant off potential, mV

i_o = corrosion current, μA

Z' = real part of impedance diagram, ohms

$-jZ''$ = imaginary part of impedance diagram, ohms

T = absolute temperature, °K

t = temperature, °C

1. INTRODUCTION

The pH of non-carbonated concrete is in a range of 12 to 13. Under this high alkaline environment, a cohesive oxide film is formed on the surface of embedded reinforcing steel to protect the steel against corrosion.

Chloride ions destroy the passivity of the steel and corrosion is likely to proceed if moisture and oxygen availability are such as to support corrosion. The depassivation process probably involves iron-chloride complexing (1): chloride ions combine with iron to form ferrous chloride at anode region. In the presence of moisture and oxygen, the ferrous chloride is subsequently converted into ferrous hydroxide and insoluble hydrous iron oxides (rust).

Chloride may be introduced in concrete from different sources such as chloride containing admixtures, chloride bearing aggregates, or de-icing salt solution permeating through hardened concrete. The free chloride present in concrete is less than the total chloride content because some of the chloride is bound by either formation of chloroaluminate or within aggregate particles. To initiate corrosion, free chloride ions must be present in a sufficient concentration in the vicinity of the steel.

Two types of corrosion cells, microcell and macrocell, are responsible for the corrosion of steel in a bridge deck.

A microcell is developed when anodes and cathodes are formed alternately along the same rebar in very close proximity to each other. For such a cell, only the mixed corrosion potentials of the anodes and cathodes can be measured. The linear polarization and A.C. impedance techniques (2-14) have been used in laboratory studies (15-19) to examine this type of corrosion.

In a macrocell, anode and cathode regions are formed some distance apart, such as a rebar electrically connected to another rebar in a less corrosion inducing environment, and both the anodic and cathodic potentials are known. This kind of corrosion can result from differential chloride concentration levels within the concrete (1,20). For instance, a rebar of the upper reinforcing mat in chloride-contaminated concrete layer may undergo active corrosion if electrically connected to the lower mat in chloride-free concrete. In the laboratory, the corrosion rate of a macrocell can be determined by direct measurement of the current flow between the anode and cathode.

Only a small amount of work has been reported in the literature with specific reference to: (1) the maximum concentration of chloride which can be accommodated before unacceptable corrosion rates are likely, (2) the available chloride for corrosion from both chloride contained in aggregates and from chloride incorporated in fresh concrete as admixtures, and (3) macrocell corrosion action due to differential chloride concentration levels within concrete.

The scope of this investigation was:

1. to determine the influence of chloride in admixed calcium chloride dihydrate on microcell corrosion and the chloride corrosion threshold value

2. to examine the effect of chloride contained in two types of chloride bearing aggregates on microcell and macrocell corrosion

3. to study the influence of differential chloride concentration levels within concrete on macrocell corrosion

4. to examine the effect of chloride in admixed calcium chloride dihydrate and chloride bearing aggregates on the alkalinity of concrete

2. EXPERIMENTAL WORK

2.1 Specimens

Test specimens for microcell measurement were 64 x 300 x 400 mm concrete slabs. Three 13 mm diameter mild steel rods were embedded 250 mm in concrete and centred 32 mm from the top surface of each slab. The rod located at the centre of the slab was used as a counter electrode, and the other two rods, which were placed 144 mm on each side of the centre rod, were working electrodes. Prior to casting, 240 mm of the embedded length of each rod was machine polished, giving a total area of 9740 mm^2; and the protruding section of the rod was painted with metal primer to a depth of 10 mm in the concrete.

Two series of microcell slabs were prepared (Table 1). Eight sets of slabs were made with admixed calcium chloride dihydrate in series 1 and 2 sets of slabs were made with 2 types of chloride bearing aggregates in series 2. A typical slab is shown in Fig 1.

Macrocell test specimens were 64 x 300 x 400 mm concrete slabs each containing an anode steel, a cathode steel, and a centre rod. The anode steel and centre rod were the same as the rods used in the microcell slabs. The cathode steel was made up of a 13 mm diameter mild steel rod welded to a 6 x 50 x 200 mm mild steel plate so that the surface area ratio of anode to cathode was 1 to 3.3. Mill scale on the cathode steel was not removed. All the steel elements were centred 32 mm from the top surface of the slab and the anode and cathode steel were placed 144 mm on each side of the centre rod.

Two series of macrocell slabs were also prepared (Table 2). The first series consisted of 3 sets of slabs. Each slab was cast in two parts at a same time: the first half, in which the anode steel was embedded, was made with admixed calcium chloride dihydrate; and the second half, in which the cathode steel was placed, was made with admixed calcium chloride dihydrate of relatively low concentration or without calcium chloride dihydrate. The second series comprised 2 sets of slabs. For these slabs, the anode blocks and cathode blocks were made with the chloride aggregates and chloride-free aggregate respectively.

CSA Type 10, normal Portland cement (with 0.003% chloride ion content), natural siliceous sand, and distilled water were used for all the mixes. Chemical composition of the cement and mix design for the concretes are shown in Tables 3 and 4.

After curing, the anode and cathode steel in some macrocell slabs were electrically coupled using an electric wire with a 50-ohm resistor. A switch was incorporated in the circuit and was activated to electrically connect the anode and cathode. A representative slab is shown in Fig 2.

At a later stage, some of the macrocell slabs were modified so that the distance between anode and cathode steel in each slab was 100 mm. This was done by cutting away the centre portion of the slab. The anode and cathode blocks were connected by mortar after cutting. Such a slab is shown in Fig 3.

2.2 Storage and Test Schedule

All the slabs were initially cured in sealed plastic sheets at about 22°C for 14 days. One half of the slabs were then stored at an outdoor site (Fig 4). Corrosion and electrical impedance measurements were taken every month. The remainder of the slabs were stored in laboratory air for 28 days after curing and were subsequently subjected to an alternate wet and dry cycle - soaking in aerated water for 3 days and drying in laboratory air for 11 days (Fig 5). Corrosion and resistance measurements were taken at every 3 and 14 days.

At a later stage, two sets of microcell slabs were oven dried at 100°C for about 14 days and then alternately soaked in aerated water for 14 days followed by drying in laboratory air for 14 days. Thereafter, these slabs were exposed to the same cycles of oven drying, water soaking, and air drying again.

During the test period, the range of indoor temperature was from 16 to 26°C and the outdoor temperature varied from 2 to 31°C. For the indoor slabs, the protruding sections of the rods near the concrete surfaces were covered by plastic caps and silicon in order to minimize corrosion at this area during the soaking period.

Only the linear polarization technique was used for the foregoing corrosion measurements for the microcell samples. After the slabs were approximately 2 years old, a number of corrosion measurements were conducted on 3 microcell slabs using the A.C. impedance technique. These slabs were previously subjected to the oven dried cycle and were made with admixed 1% calcium chloride dihydrate (CF2), 2% calcium chloride dihydrate (CH2), and chloride aggregate 2 (CK1).

Prior to A.C. impedance testing, the slabs were stored at 80°C for 4 days. Slab CH2 was subsequently soaked in water for 1 day followed by drying in air at room temperature the next day. It was then sealed with a polyethylene sheet for 4 days in order to reduce the nonuniform moisture distribution within the slab. After oven drying, both slabs CF2 and CK1 were submerged in water for 9 days followed by sealing with polyethylene. During the test, all the slabs were kept wrapped in polyethylene. One cycle of measurement (10 mHz - 10 kHz) was obtained from slab CH2 and 9

cycles of measurements were obtained from slabs CF2 and CK1. Test temperature was maintained at about 23°C.

Some of the rods were removed from typical microcell and macrocell slabs at different test periods. A visual assessment of the corrosion was conducted. In addition, the mass loss of a set of rods in the microcell slabs were determined gravimetrically after the slabs were exposed to two complete oven dried cycles.

At the end of the test stage, chloride and pH in the vicinity of the rods were measured from a series of concretes. The slabs were initially cut along the rods, and the pH levels of the concretes were measured immediately using pH indicators. A 25 x 25 x 100 mm concrete core was then cut from each of the slabs for chloride analysis.

2.3 Concrete Resistivity Measurement

AC resistances between the adjacent rods in the slabs were measured by a Gen Rad RLC-Digibridge impedance meter. The resistance readings were subsequently converted to resistivities by multiplying the resistances by a calibration factor (1). For the macrocell slabs, the resistance readings were taken when the anodes and cathodes were electrically disconnected.

To determine the calibration factors for both the 64 x 300 x 400 mm slabs and mortared slabs, four epoxy-coated plywood boxes were made. These boxes contained the same rebars which were arranged in the identical patterns as those in the slabs. Each box was filled with a 2.2% calcium bromide solution and subjected to different temperatures ranged from 5 to 30°C. Electrical resistivity of the solution, which was obtained by a standard resistivity electrode, and resistance between the adjacent rods were recorded at various temperatures. The calibration factor (ratio of the measured resistivity to resistance) at each temperature was determined. The average values of the calibration factor for the 64 x 300 x 400 mm slabs and the mortared slabs were 17 and 24 ohm-cm/ohm respectively.

The relationship between concrete resistivities at different temperatures was obtained using Hinrichson-Rasch Law

$$\rho_{c1} = \rho_{c2} \; e^{a\left(\frac{1}{T_1} - \frac{1}{T_2}\right)} \qquad (1)$$

where ρ_{c1} and ρ_{c2} are the concrete resistivities at absolute temperatures T_1 and T_2 respectively, and `a' is a constant. A value of 2900 (21) was used for `a' in this study.

The effect of temperature on corrosion current, io , was determined by the expression (1)

$$io_1 = \frac{io_2}{e^{a\left(\frac{1}{T_1} - \frac{1}{T_1}\right)}} \qquad (2)$$

where io_1 and io_2 are the corrosion currents at absolute temperatures T_1 and T_2, and 'a' is the same constant in equation 1.

2.4 Corrosion Measurement

Corrosion of the microcell specimens was examined by the linear polarization and A.C. impedance techniques.

In the linear polarization measurement, corrosion rates of the test rods were determined using Stern and Geary equation with an assumed value of 100 mV for the anodic and cathodic Tafel slopes and the experimentally obtained values of polarization resistance, R_p. The procedure to obtain R_p was: corrosion potential, E_o, of a test rod was measured with respect to a copper/copper sulfate half cell. This value of E_o was set on a EG & G 363 potentiostat and the steel was then polarized by overpotentials of 4 mV and 8 mV for 1 msec from a signal generator. The induced currents were recorded on a Tektronix T912 oscilloscope. R_p was equal to the slope of the plot of overpotentials versus the induced currents.

A.C. impedance data were obtained using a Solartron 1170 Frequency Response Analyser and a Solartron 1186 Electrochemical Interface. The data were analysed on a Zenith Z 151 microcomputer. Real and imaginary parts of the cell impedance and the corresponding impedance spectrum were recorded on a printer. A 10 mV perturbing sinusoidal signal with a selected frequency range from 10 mHz to 10 kHz was applied to the test specimens.

Corrosion currents in the macrocell slabs were determined by Ohm's Law. The potential drops across the small resistors incorporated in the connection between anodes and cathodes were obtained using a HP 3465A digtal multimeter. The resistors were chosen so that their resistances were less than 10% of the concrete resistances between the anodes and cathodes. The corrosion currents were equal to the measured voltage drops divided by the measured value of the resistance over which the voltage drop occurred.

3. RESULTS

A summary of the test results are shown in Tables 5 to 9 and Figs 6 to 17.

All the concrete resistivity data were obtained from the AC resistance readings measured by parallel equivalent circuit with 1 kHz frequency. The corrosion current data for the microcell specimens were determined using the linear polarization method.

Typical results of the influence of storage condition on corrosion currents, steel potentials, and concrete resistivities for the microcell slabs are shown in Figs 6 and 7.

Six sets of concrete resistivity, steel potential, and corrosion current data for the indoor microcell slabs are listed in Tables 5 to 7 for comparison purpose. The data for the slabs subjected to the 3 day/11 day wet/dry cycle were taken at the ends of the soaking periods and the data for the slabs exposed to the oven dried cycle were obtained when the corrosion currents in the slabs reached their `apparent´ peak levels (some of the corrosion current data may not be the actual maximum values since the corrosion measurements were not conducted every day during the water soaking period). All the concrete resistivity and corrosion current data have been adjusted to an arbitrary temperature of 21°C.

Figure 8 shows the relationship between corrosion current and admixed chloride content. The currents were the average corrosion currents in the slabs exposed to 2 complete oven dried cycles.

The experimentally obtained A.C. impedance diagrams for the rods in typical admixed chloride and chloride aggregate slabs, as well as their corresponding theoretical impedance diagrams, are shown in Figs 9 and 10. The high frequency portion of the impedance spectrum in Fig 10 (circled zone) is shown enlarged in Fig 11.

The corrosion on the rods in representative microcell slabs are shown in Figs 12 and 13. The rods were in the slabs stored outdoors for 2 years and the slabs exposed to 4 complete oven dried cycles.

Comparison of the electrochemical and gravimetric mass loss for a set of rods embedded in the slabs subjected to 2 complete oven dried cycles is given in Table 8. The electrochemical mass loss data were obtained from the average corrosion current data in Fig 8.

Figure 14 shows the corrosion currents in all 5 types of indoor macrocell slabs during the test stage.

Figure 15 shows the effect of storage condition on corrosion currents, anode/cathode potential differences, and concrete resistivities for the 2% chloride to chloride-free macrocell slabs. The potential difference data were obtained immediately after the anode and cathode steel were electrically disconnected.

The corrosion on the rods in typical macrocell slabs is shown in Fig 16. The rods were removed from the outdoor slabs after 2 years of exposure.

Measured chloride contents of the concrete adjacent to the reinforcing steel for the oven dried slabs is given in Table 9 and Figure 17. These chloride contents were obtained on prisms 25 x 25 x 100 mm cut from the slabs after bar removal and subsequently ground in preparation for the total and water soluble chloride determinations.

4. DISCUSSION

4.1 Measured Chloride Contents

As shown in Fig 17, both the total and soluble chlorides are more or less linear functions of the admixed chloride. It is likely that some chlorides were leached from the slabs during the prolonged test period and there was a redistribution of chlorides within each slab. This likely resulted in the deviation of the individual chloride quantites from the best fit curves.

As far as chloride threshold values are concerned it is recommended that 0.2, 0.4 and 0.6% admixed calcium chloride dihydrate be considered to be the equivalent of 0.014, 0.022 and 0.030% soluble chloride ions by mass of concrete.

4.2 Microcell Specimens

4.2.1 Indoor Slabs

1. Concrete Resistivity

Electrical resistivities of all the concretes increased steadily with age (Table 5). The resistivities for the wet mature concretes subjected to the 3 day/11 day wet and dry cycle were mostly over 10,000 ohm-cm, which has been suggested as a critical resistivity value to support corrosion (22).

The resistivities for the concretes containing admixed chlorides decreased with increase in chloride content. This was probably because ionic activity in the pore solution of the cement pastes increased with increasing concentration of chloride ion.

The resistivity for the concrete made with chloride aggregate 1 was lower than that for the concrete made with chloride aggregate 2 although the chloride ion content in aggregate 1 was only about 70% of that in aggregate 2. For both these concretes the gain in resistivity with age was relatively fast compared to the admixed chloride concretes (Table 5). These results indicated that the mobility of the chloride in the chloride aggregate concretes appeared to be significantly less than that in the admixed chloride concretes probably due to the bonding effect. This is an important aspect of corrosion if only free chloride is the corrosion agent.

When the oven dried slabs were soaked in water, the concrete resistivities dropped considerably (Fig 7). The lowest resistivities for most of the concretes occurred a few days after soaking had been started and were well below 10,000 ohm-cm. The resistivities then increased steadily in the remaining soaking period and rose rapidly during drying in air. These downward and upward movements of concrete resistivity were also observed when the slabs were subjected to the following alternate wet and dry cycle though the effect was not as marked. A similar trend was also found in the subsequent oven dried cycles except the changes in resistivity due to drying and wetting were smaller than those in the initial cycle.

2. Steel Potential

Corrosion potentials of the rods embedded in the slabs subjected to 3 day/11 day wet and dry cycle generally decreased with time. The steel potentials in the mature slabs varied from about -100 mV to -250 mV (Table 6). There was no clear relationship between the steel potentials and chloride content in concrete when the admixed calcium chloride dihydrate was less than 1.0%. However, the steel potentials became more negative as the admixed chloride content increased when the slabs were exposed to the oven dried cycle.

The potentials of the rods in the chloride aggregate slabs were comparable to those in the chloride-free and 0.2% admixed chloride slabs.

The steel potentials became more negative after the oven dried slabs were soaked in water. In general, the most negative steel potentials occurred in the first few days after the soaking had been commenced. In the first cycle, these potential values were from about -350 mV for the chloride-free slabs to -600 mV for the 2% admixed chloride slabs. These changes in steel potentials were likely caused by the increased oxygen concentration at the steel and concrete interface and the redistribution of chloride ions. The steel potentials were less negative in the subsequent oven dried cycles than those in the first one.

3. Linear Polarization Corrosion Assessment

Test results obtained from the linear polarization method showed the following:

Corrosion currents in all the slabs subjected to the 3 day/11 day wet and dry cycle decreased with age.

Average corrosion currents in the chloride aggregate slabs over the test period were comparable to the corrosion current in the 1% admixed chloride slabs.

Corrosion currents in the slabs increased considerably after the oven dried slabs were submerged in water (Table 7). The peak currents usually occurred when the concrete resistivities reached minimum levels and were about 5 to 10 times the corrosion currents before the slabs were oven dried. In the remaining wet and dry period and the subsequent oven dried cycles, the corrosion currents were also inversely related to the concrete resistivity.

Corrosion currents in the admixed chloride slabs generally increased with increasing chloride content. As shown in Fig 8, there was a marked increase in the average corrosion currents in the slabs subjected to the oven dried cycle when admixed chloride content increased to 0.4 or more. Based on this set of data, the chloride corrosion threshold limit was probably between 0.2% and 0.4% calcium chloride dihydrate by mass of cement (0.014 and 0.022% chloride ion by mass of concrete).

4.2.2 Outdoor Slabs

The concrete resistivities, steel potentials, and corrosion currents measured by the linear polarization method in the outdoor slabs showed

similar trends to those of the indoor slabs subjected to the 3 day/11 day wet and dry cycle. However, greater changes in both concrete resistivities and corrosion currents were observed due to a wide variation of outdoor temperature.

4.2.3 A.C. Impedance Corrosion Assessment

As shown in Fig 9, the A.C. impedance spectrum consisted of a part of a semicircle at high frequencies (10 Hz to 10 kHz) and a straight line at low frequencies (10 mHz to 1 Hz). It can be seen that the semicircular portion was depressed and the slope at low frequencies is less than 45°. This was probably due to the heterogeneous property of the steel surface and perhaps the simultaneous occurrence of both microcell and macrocell corrosion phenomena. From Fig 9, the electrolyte resistance, R_e, was about 86 ohms, and the charge transfer resistance, R_t, which was given by the chord of the depressed semicircle, was about 11 ohms.

In Fig 10, the impedance spectrum was dominated by a steep curve (with slope greater than 45°) at low frequencies. This curve is the first portion of the large semicircle formed at low frequencies for an electrode with a passive film formed on its surface. The high frequency portion of the spectrum (the circled zone) is shown enlarged in Fig 11. It is clear that the smaller semicircle was formed only within a small range of frequencies (1 kHz - 8 kHz). R_e and R_t were estimated to be 380 ohms and 26 ohms respectively, and the passive film resistance, R_f, had a very high value.

These findings showed that the steel in the 2% admixed chloride slab experienced active corrosion and the corrosion rate was diffusion controlled. The steel in the chloride aggregate slab, however, was passivated and not corroding.

It should be noted that the result for the steel in the chloride aggregate slab obtained by the A.C. impedance technique was contrary to that obtained from the linear polarization method. A.C. impedance indicated negligible corrosion of the chloride aggregate concrete whereas linear polarization experiments suggested significant corrosion was taking place.

4.2.4 Visual Inspection

Inspection of the test rods indicated the following:
The corrosion on the steel embedded in the outdoor slabs and the indoor slabs subjected to the 3 day/11 day wet and dry cycle was comparable.

After 2 years of outdoor exposure, there was only little corrosion on the steel in the admixed chloride slabs with chloride content 0.6% or less. The corrosion increased quite markedly when admixed chloride increased to 0.8% (Fig 12). The steel in the chloride aggregate slabs showed very little corrosion.

Most of the steel removed from the admixed chloride slabs subjected to the oven dried cycle showed substantial corrosion as seen in Fig 13. The corrosion increased with increasing chloride content in concrete. The

chloride corrosion threshold for these slabs was probably between about 0.2% and 0.4% calcium chloride dihydrate by mass of cement (0.014% and 0.022% chloride ion by mass of concrete). For the steel in the slabs with relative high admixed chloride content (0.8 to 2.0%), severe pittings were found on the steel surfaces. The numbers and sizes of the rust pits increased with increase in chloride content. When many of these slabs were cut open, black corrosion products ($Fe_3O_4 . 3\ H_2O$) and, in some cases, dark green corrosion products ($FeCl_2$) were seen initially on the steel and concrete interface. Upon exposure to laboratory air, these corrosion products soon converted to red-yellow brown rust ($Fe_2O_3 . 3H_2O$).

Only a small quantity of rust could be seen on the steel removed from the chloride aggregate slabs subjected to the oven dried cycle (Fig 13). The rods were nearly corrosion-free. This result was in good agreement with that obtained from the A.C. impedance method. It also showed that, using Tafel slopes of 100 mV/decade, the linear polarization technique greatly overestimated the actual corrosion rates of the steel for the chloride aggregate slabs.

Table 8 shows that the differences in the mass loss determined from the linear polarization technique and gravimetric method were within a factor of one-half to two for the steel in the admixed chloride slabs exposed to the oven dried cycle. However, for the steel in the chloride aggregate slabs, the mass loss calculated electrochemically was significantly higher than that obtained gravimetrically.

From the foregoing results, the chloride in the two types of chloride bearing aggregates appeared to be bound and was not significant in the corrosion process.

4.3 Macrocell Specimens

Electrical potential differences of the anode and cathode steel in the indoor and outdoor macrocell slabs changed continuously during the test period. Among the 5 types of slabs, the anode/cathode potential differences in the slabs made with 2% admixed chloride and chloride-free concrete (CM) were the largest and remained positive, while those in the other slab series were small or negative most of the time.

Except in the slabs CM, the steady corrosion currents in the test slabs were small (Fig 14). The measured corrosion currents were usually directly proportional to the instant off anode/cathode potential differences but inversely proportional to the concrete resistivities.

On the slabs made with 1% and 2% admixed chloride concrete (CN), the corrosion currents were small even though the concrete resistivity was relatively low (about 90% of the concrete resistivity for slab CM). The low macrocell corrosion rates apparently resulted from the small anode/cathode potential differences in such slabs. These results show that, for a given range of concrete resistivity, anode/cathode potential difference is a dominating factor controlling the corrosion rate of a macrocell. The potential difference, in turn, can be affected by differential concentration of chloride ions in anode and cathode region.

In most cases, the corrosion currents in the mortared slabs were higher than those in the large slabs due to the lower resistance between the anodes and cathodes.

Figure 16 shows corrosion on a set of anode steel in the slabs stored outdoors for 2 years. It can be seen that corrosion on the steel in slab CM was the most severe and the steel in the chloride aggregate slabs showed very little corrosion.

Noted that the method used to determine the corrosion currents in the macrocell slabs only indicated the galvanic actions of the anode and cathode steel. It gave no information on the possible self corrosion of the anode steel. The actual corrosion rates of the anode steel were likely to be the combination of both the microcell and macrocell corrosion.

4.4 Alkalinity

The pH of the concretes were in a range of about 12.0 to 12.5 regardless of the admixed chloride content and types of aggregates used. The pH of the corrosion products, on the other hand, varied from 5 to 9. When a rebar embedded in concrete undergoes active corrosion, corrosion products are likely to form at the concrete-steel interface. The pH at the anode region would be well below the normal protective range for the embedded steel. This, in turn, can facilitate further corrosion.

5. CONCLUSIONS

The test results of this investigation showed that:

1. Corrosion rates of the single steel rods embedded in the concretes increased with increase in admixed chloride content. The chloride corrosion threshold limit appeared to be between 0.2% and 0.4% calcium chloride dihydrate by mass of cement (0.014% and 0.022% by mass of concrete).

2. For a given range of concrete resistivities, macrocell corrosion rates of the electrically connected steel embedded in the concretes were dependent on the differential concentration of chloride ions in the anode and cathode regions; large difference in chloride concentration levels resulted in high corrosion rates.

3. The chloride in the chloride bearing aggregates used for this investigation was not available, to any significant degree, for the corrosion process.

4. The pH of the concretes were in a range from 12 to 12.5 regardless of the admixed chloride content and types of aggregates used in the mixes.

REFERENCES

1. Clear, K.C., "Cost Effective Rigid Concrete Construction and Rehabilitation in Adverse Environments," FCF Annual Progress Report, Project No. 4K, 1981.

2. Stern and Geary, "A Theoretical Analysis of the Shape of Polarization Curves," Journal of the Electrochemical Society, Vol. 104, 1957, pp.56-63.

3. Mansfield, F., "Tafel Slopes and Corrosion Rates from Polarization Resistance Measurements," Corrosion, NACE, Vol. 29, 1973, pp.397-402.

4. Jones, D.A., and Greene, N.D., "Electrochemical Measurement of Low Corrosion Rates," Corrosion, NACE, Vol. 22, 1966, pp.198-205.

5. Prazak, M., "The Polarization Resistance Method for Corrosion Testing," Werkstoffe and Korrosion, Vol. 25, 1974, pp.104-112.

6. Heitz, E., and Schwenk, W., "Theoretical Basis for the Determination of Corrosion Rates from Polarization Resistance," British Corrosion Journal, Vol. 11, 1976, pp.74-77.

7. Callow, L.M., Richardson, J.A., and Dawson, J.L., "Corrosion Monitoring Using Polarization Resistance Measurements: I. Techniques and Correlations, and II. Sources of Error," British Corrosion Journal, Vol. 11, 1976, pp.123-139.

8. Jones, D.A., "Polarization in High Resistivity Media," Corrosion Science, Vol. 8, 1968, pp.19-27.

9. Doig, P., and Flewitt, P.E.J., "Simultaneous Correction of the IR Potential Drop during Potentiostatic Polarization Measurements," British Corrosion Journal, Vol. 11, 1976, pp.78-79.

10. Hubbe, M.A., " Polarization Resistance Corrosivity Test with a Correction for Resistivity," British Corrosion Journal, Vol. 15, 1980, pp.193-197.

11. Stern, M., and Weisert, E.D., "Experimental Observations on the Relation between Polarization Resistance and Corrosion Rate," Proceedings, ASTM, Vol. 59; 1959, pp.1280-1290.

12. Armstrong, R.D., Bell, M.F., and Metcalfe, A.A., "The A.C. Impedance of Complex Electrochemical Reactions," Special Periodical Reports - Electrochemistry, Vol. 6, 1978, pp.98-127.

13. Hladky, K., Callow, L.M., and Dawson, J.L., "Corrosion Rates from Impedance Measurements: An Introduction," British Corrosion Journal, Vol. 15, 1980, pp.20-25.

14. Gabrielli, C., "Identification of Electrochemical Processes by Frequency Response Analysis," Solarton Instruments, Technical Report Number 004/83, Farnborough, England, 1983.

15. Escalante, E., Ito, S., and Cohen, M., "Measuring the Rate of Corrosion of Reinforcing Steel in Concrete," National Bureau of Standards, NBSIR 80-2012, 1980.

16. Andrade, C., and Gonzalez, J.A., "Quantitative Measurements of Corrosion Rate of Reinforcing Steels Embedded in Concrete Using Polarization Resistance Measurements," Werkstoffe und Korrosion, Vol. 29, 1978, pp.515-519.

17. Gonzalez, J.A., Algaba, S., and Andrade, C., "Corrosion of Reinforcing Bars in Carbonated Concrete", British Corrosion Journal, Vol. 15, 1980, pp.135-139.

18. Rosenberg, A.M., and Gaidis, J.M., "Methods of Determining Corrosion Susceptibility of Steel in Concrete," Transportation Research Record 692, Transportation Research Board, 1978, pp. 28-34.

19. John, D.C., Searson, P.C., and Dawson, J.L., "Use of AC Impedance Technique in Studies on Steel in Concrete in Immersed Conditions," British Corrosion Journal, Vol. 16, 1981, pp.102-106.

20. Lewis, D.A., and Copenhagen, W.J., "Corrosion of Reinforcing Steel in Concrete in Marine Atmospheres," Corrosion, Vol. 15, 1959, pp.382-388.

21. Ip, A.K.C., "Aspects of Corrosion of Steel in Concrete," Ph.D. thesis, Department of Civil Engineering, Queen's University, 1984, pp.125-167.

22. Brown, R.D., "Design Prediction of the Life for Reinforced Concrete in Marine and Other Chloride Environments," Durability of Building Materials, Vol. 1, 1982, pp.113-125.

TABLE 1. MICROCELL SLABS

Series	Slab No.	Calcium Chloride Dihydrate (%)+	Coarse Aggregate Type *
1	CA1 - CA6	Nil	N
1	CB1 - CB6	0.2	N
1	CC1 - CC6	0.4	N
1	CD1 - CD6	0.6	N
1	CE1 - CE6	0.8	N
1	CF1 - CF6	1.0	N
1	CG1 - CG6	1.5	N
1	CH1 - CH6	2.0	N
2	CJ1 - CJ6	Nil	1
2	CK1 - CK6	Nil	2

TABLE 2. MACROCELL SLABS

Series	Slab No.	Calcium Chloride Dihydrate (%)+		Coarse Aggregate Type *	
		Anode Block	Cathode Block	Anode Block	Cathode Block
1	CL1 - CL6	1.0	Nil	N	N
1	CM1 - CM6	2.0	Nil	N	N
1	CN1 - CN6	2.0	1.0	N	N
2	CO1 - CO6	Nil	Nil	2	N
2	CP1 - CP6	Nil	Nil	1	N

\+ % by mass of cement
* N - normal crushed limestone aggregate
1 - limestone aggregate with chloride ion content 0.136%
2 - limestone aggregate with chloride ion content 0.197%

TABLE 3. CHEMICAL ANALYSIS OF THE PORTLAND CEMENT

Chemical analysis:	%
CaO	62.7
SiO_2	20.6
Al_2O_3	4.9
MgO	3.1
SO_3	2.8
Fe_2O_3	2.7
K_2O	0.8

TABLE 4. MIX DESIGN FOR THE CONCRETE

Cement	CSA Type 10 (with 0.003% chloride ion content)
Fine aggregate	natural siliceous sand
Coarse aggregate	crushed limestone aggregate or/and chloride bearing aggregates
Mixing water	distilled water
Cement content	400 kg/m^3
Cement/aggregate/water	1.00/4.45/0.45
Slump	75 ± 25 mm
Air content	6 ± 1 %
Admixtures	Calcium chloride dihydrate (for admixed chloride slabs), water reducing agent Pozzolith 83 and air entraining agent MB-AE 10

TABLE 5. CONCRETE RESISTIVITIES FOR THE INDOOR MICROCELL SLABS

Admixed Chloride [+]	Concrete resistivity (ohm-cm)					
	3 day/11 day wet and dry cycle				Oven dried cycle	
	Days					
	45	115	220	405	1st	2nd
nil	9100	13000	18400	23300	4300	7200
0.2%	7400	13100	18100	20000	4400	5400
0.4%	7400	12400	15700	19400	3900	5100
0.6%	8500	11800	17500	19100	4600	6100
0.8%	7600	11100	16500	18300	4200	6400
1.0%	7100	11300	15500	18000	4100	6100
1.5%	6700	10600	15300	18200	4900	4700
2.0%	6000	9600	12500	15300	3400	4100
1[*]	6400	12200	14600	20400	3800	4300
2[*]	7100	12900	15000	22000	3900	4600

[+] Admixed calcium chloride dihydrate by mass of cement

[*] Chloride bearing aggregates

TABLE 6. STEEL POTENTIALS FOR THE INDOOR MICROCELL SLABS

Admixed chloride [+]	Steel potential (-mV, CSE)					
	3 day/11 day wet and dry cycle				Oven dried cycle	
	days: 45	115	220	405	1st	2nd
nil	127	207	123	121	350	194
0.2 %	118	224	90	150	459	295
0.4 %	100	141	191	129	428	371
0.6 %	99	109	129	100	457	396
0.8 %	212	179	119	120	472	418
1.0 %	224	248	126	102	523	435
1.5 %	241	313	203	179	478	470
2.0 %	324	306	258	254	586	640
1*	139	150	183	58	344	258
2*	135	125	82	67	339	274

[+] Admixed calcium chloride dihydrate by mass of cement

* Chloride contaminated aggregates

TABLE 7. CORROSION CURRENTS IN THE INDOOR MICROCELL SLABS

Admixed chloride [+]	Corrosion currents (μA)[Δ] 3 day/11 day wet and dry cycle				Oven dried cycle	
	days:45	115	220	405	1st [o]	2nd [o]
nil	301	231	125	78	980	674
0.2 %	319	187	117	110	886	674
0.4 %	343	205	146	120	767	660
0.6 %	317	248	140	126	766	599
0.8 %	355	245	159	138	824	563
1.0 %	462	257	155	140	999	852
1.5 %	450	305	198	170	1348	973
2.0 %	511	345	225	210	1863	1244
1 [*]	490	295	200	174	1137	897
2 [*]	453	227	180	133	1142	948

[+] Admixed calcium chloride dihydrate by mass of cement

[*] Chloride bearing aggregates

[Δ] Obtained from the linear polarization method

[o] Some of the corrosion current data may not be the maximum values

TABLE 8. ELECTROCHEMICAL AND GRAVIMETRIC MASS LOSS OF TYPICAL RODS IN THE MICROCELL SLABS SUBJECTED TO THE OVEN-DRIED CYCLE

Admixed chloride [+]	Electrochemical mass loss (gm) [Δ]	Gravimetric mass loss (gm)
Nil	2.0	0.6
0.2 %	2.0	1.1
0.4 %	2.1	1.2
0.6 %	2.3	1.4
0.8 %	2.6	1.8
1.0 %	2.7	2.1
1.5 %	3.4	2.6
2.0 %	4.4	3.3
1*	2.9	0.4
2*	2.7	0.5

[+] Admixed calcium chloride dihydrate by mass of cement

[*] Chloride bearing aggregates

[Δ] Obtained from the linear polarization method

TABLE 9. MEASURED CHLORIDE CONTENTS OF THE CONCRETE

Admixed Chloride +	Chloride Content (% by mass of concrete)	
	Total	Soluble
nil	0.009	0.006
0.2 %	0.031	0.012
0.4 %	0.041	0.026
0.6 %	0.052	0.027
0.8 %	0.077	0.039
1.0 %	0.101	0.067
1.5 %	0.083	0.054
2.0 %	0.124	0.090
1 *	0.087	0.024
2 *	0.109	0.034

\+ Admixed calcium chloride dihydrate by mass of cement

* Chloride bearing aggregates

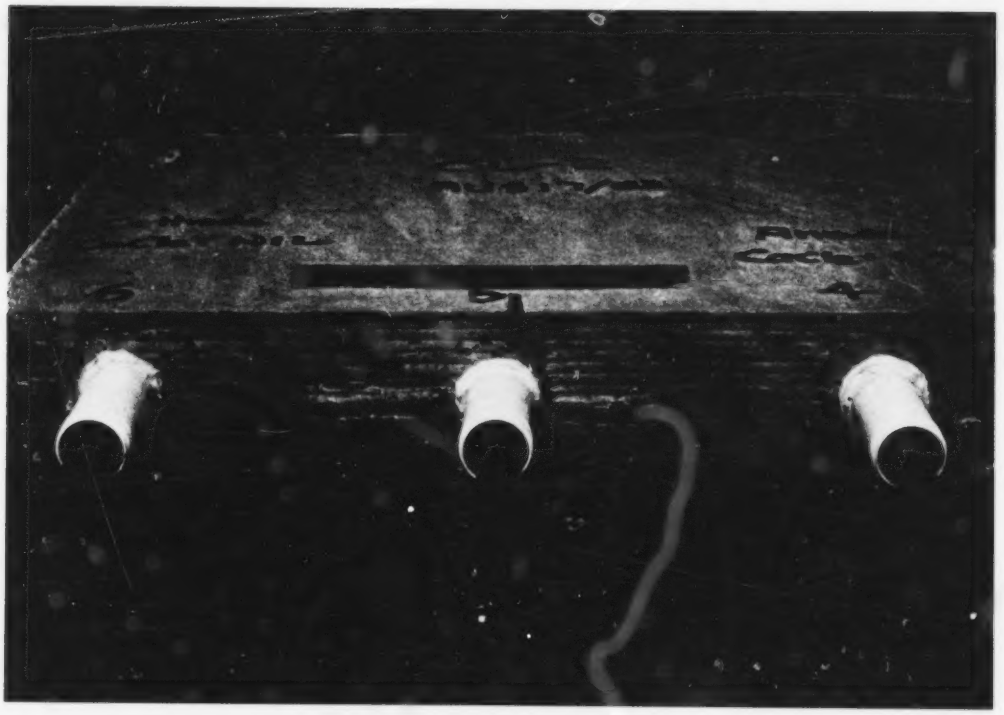

Figure 1/ Microcell Slab

Figure 2/ Macrocell Slab 1

Figure 3/ Macrocell Slab 2

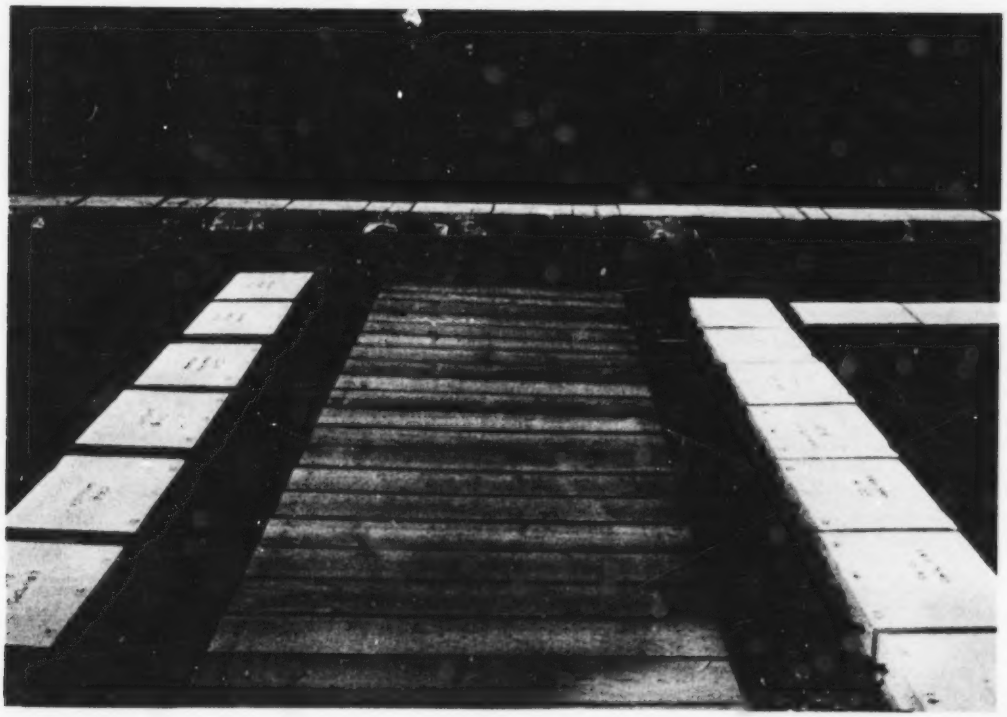

Figure 4/ Outdoor Storage

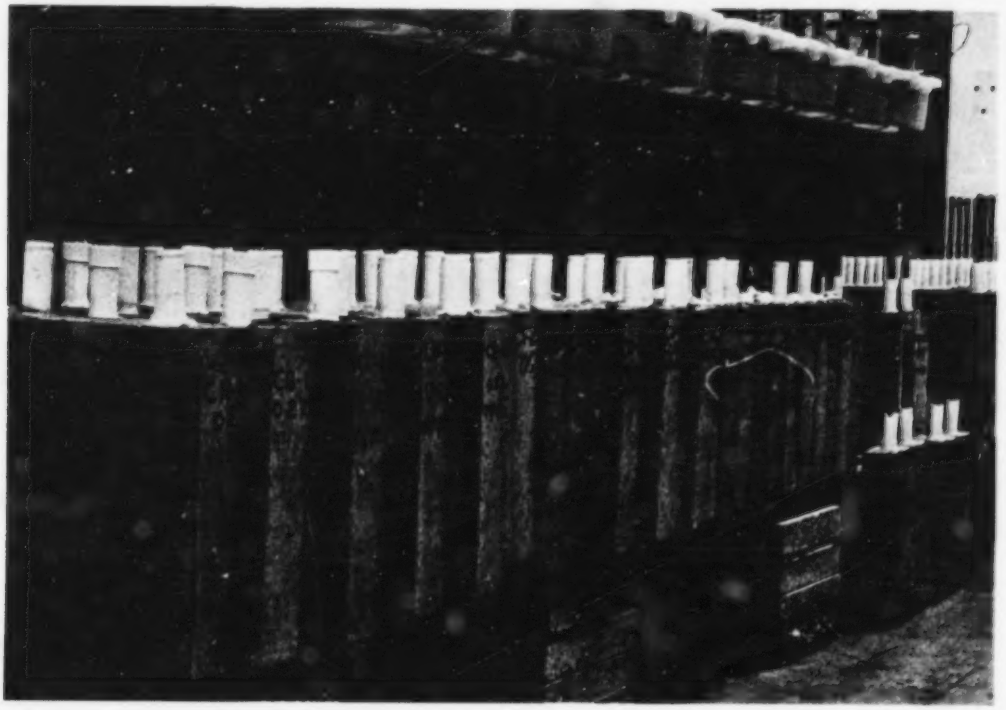

Figure 5a/ Indoor Storage – Air Drying Period

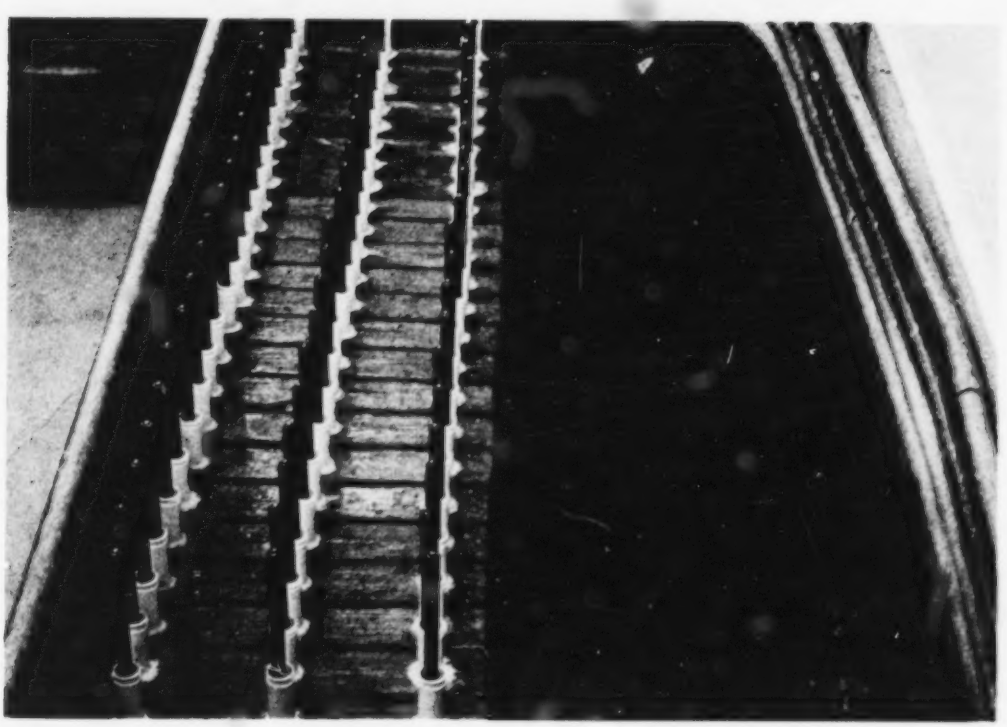

Figure 5b/ Indoor Storage – Water Soaking Period

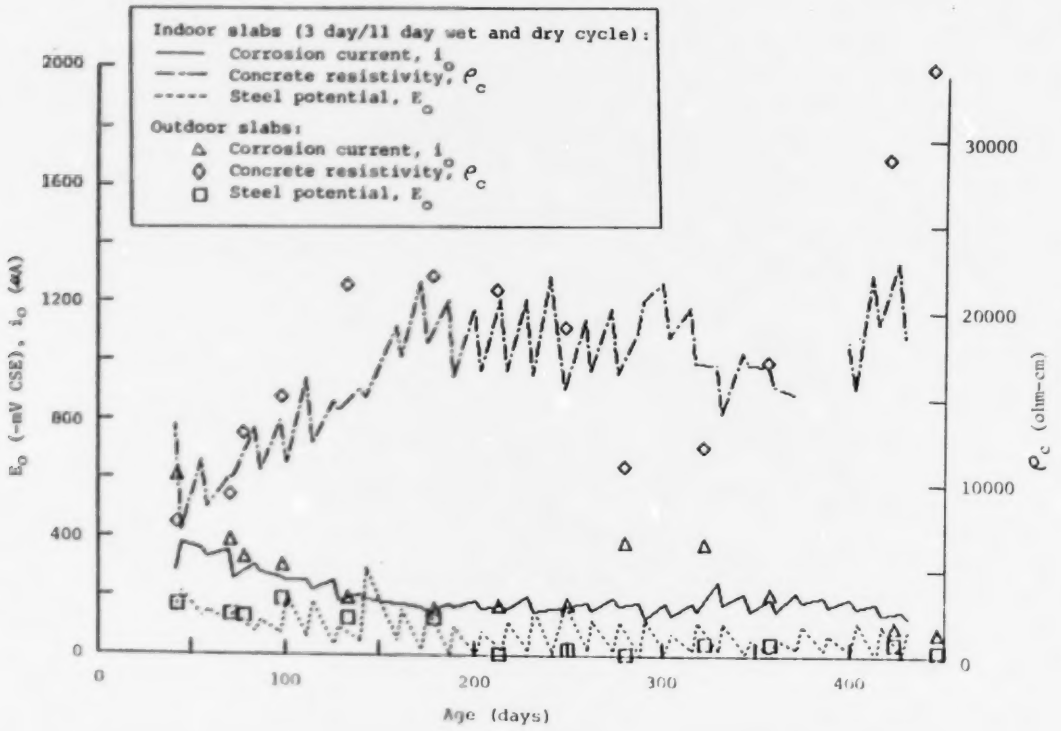

Figure 6/ Corrosion Currents, Steel Potentials, and Concrete Resistivities for the 0.8% Admixed Chloride Microcell Slabs Stored Outdoors and Subjected to the 3 Day/11 Day Wet/Dry Cycle

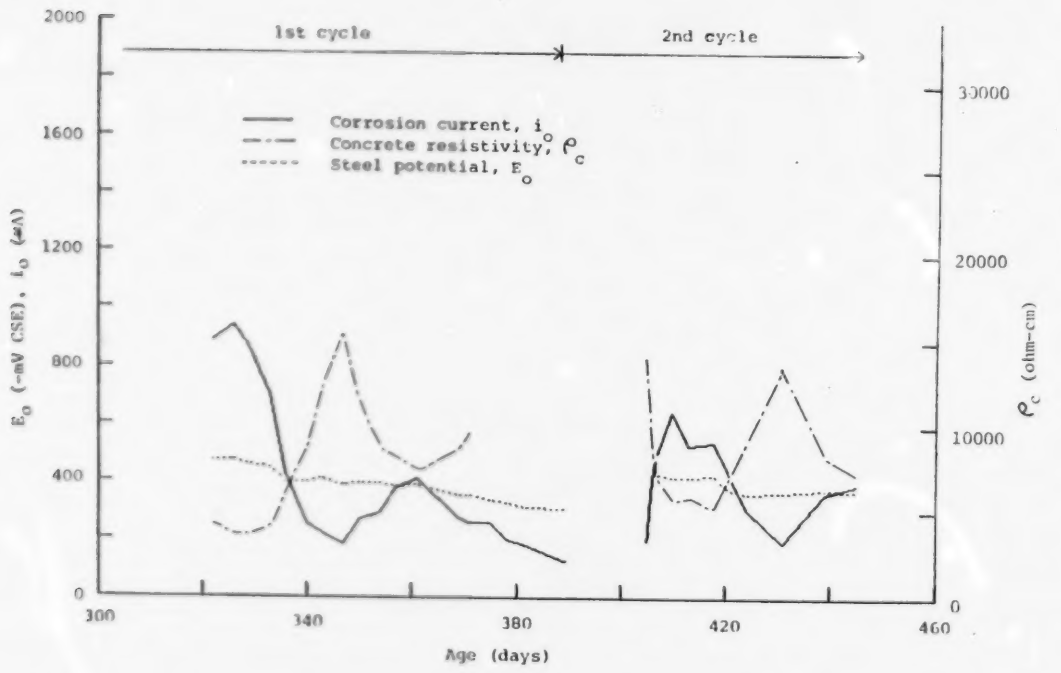

Figure 7/ Corrosion Currents, Steel Potentials, and Concrete Resistivities for the 0.8% Admixed Chloride Microcell Slabs Subjected to the Oven-Dried Cycle

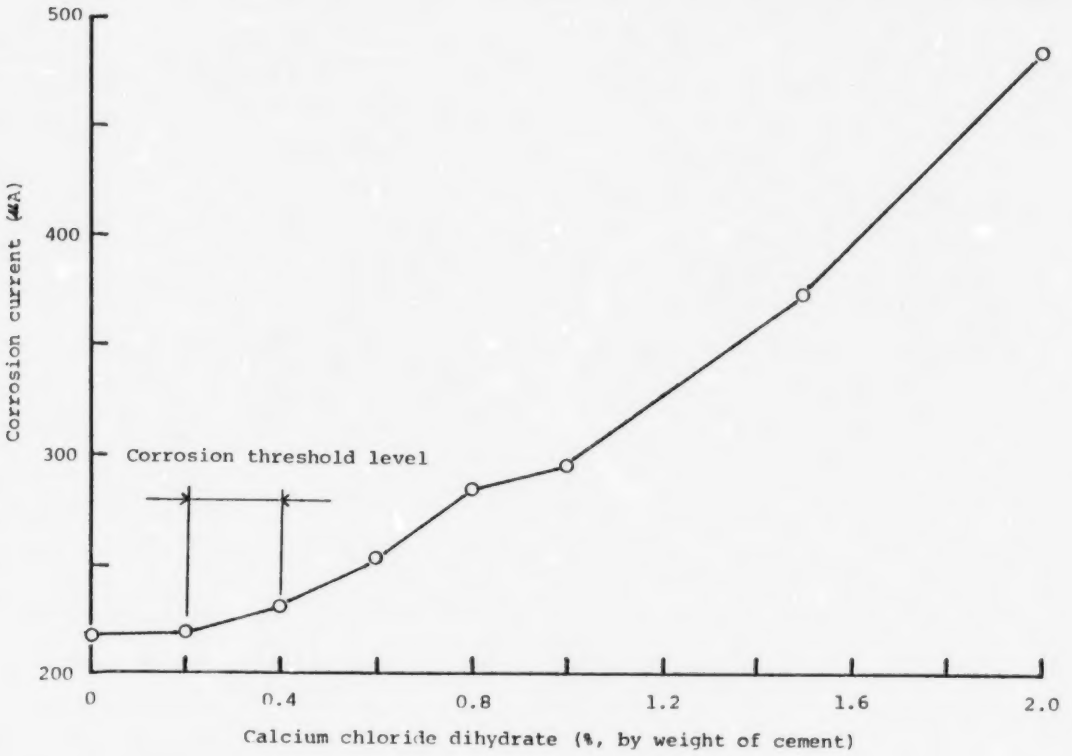

Figure 8/ Average Corrosion Currents in the Admixed Chloride Microcell Slabs Subjected to the Oven-Dried Cycle

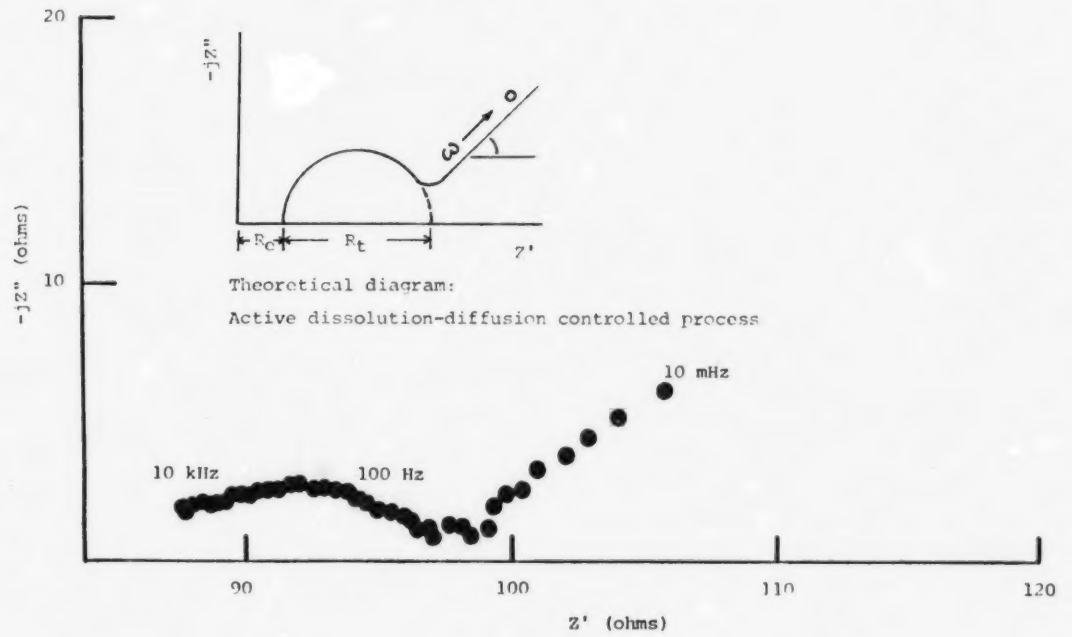

Figure 9/ Impedance Diagram for the Steel in a 2% Admixed Chloride Microcell Slab

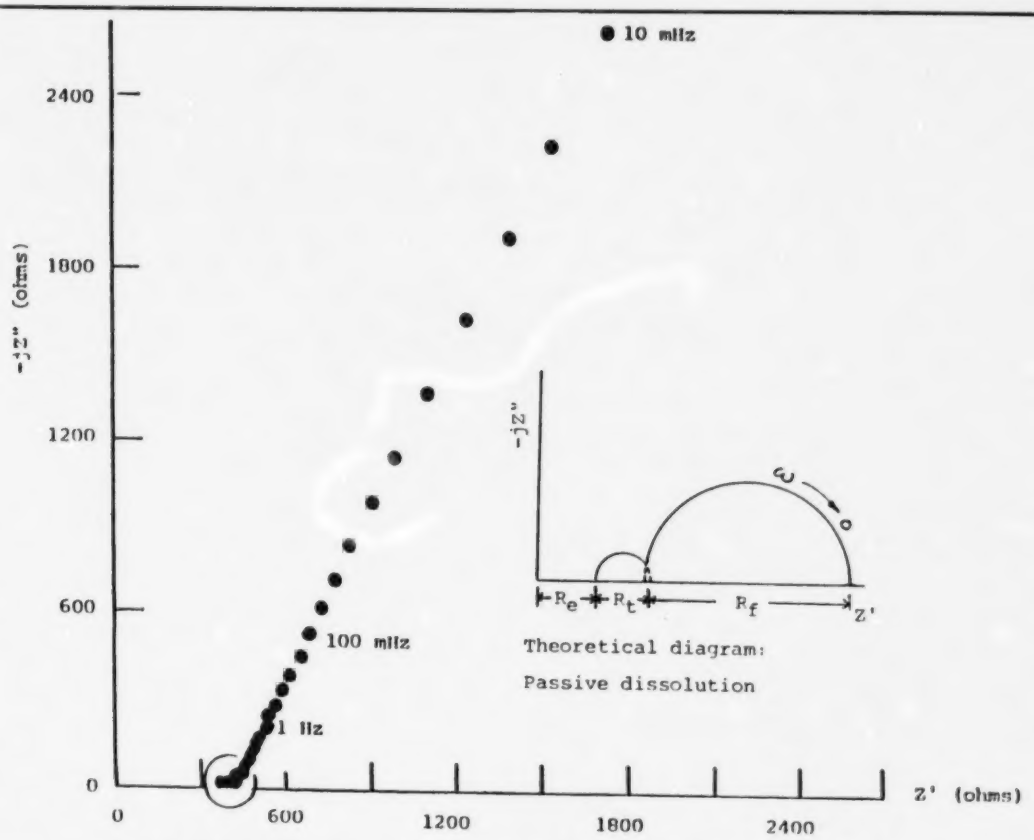

Figure 10/ Impedance Diagram for the Steel in a Chloride-Aggregate Microcell Slab

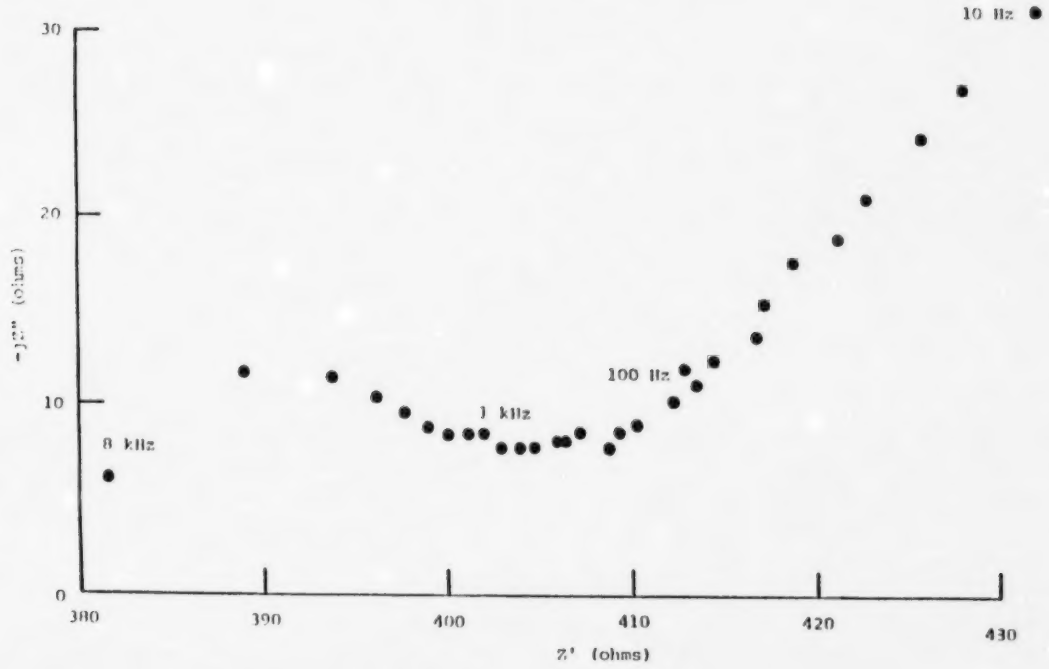

Figure 11/ Impedance Diagram for the Steel in a Chloride-Aggregate Microcell Slab at High Frequencies

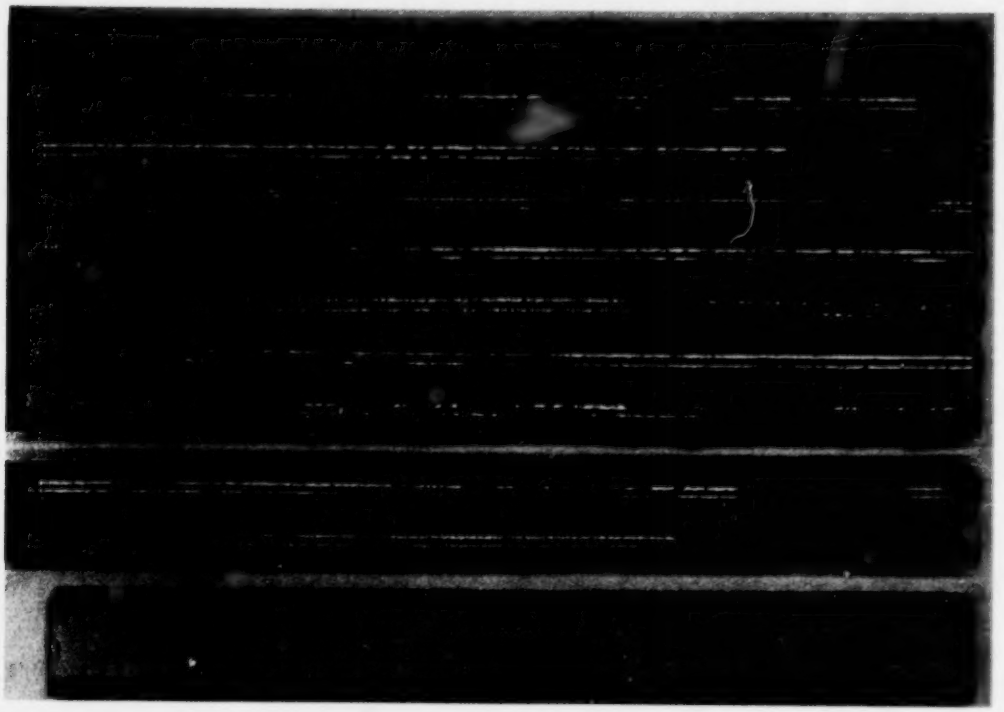

Figure 12/ Corrosion on the Steel Embedded in the Outdoor Microcell Slabs

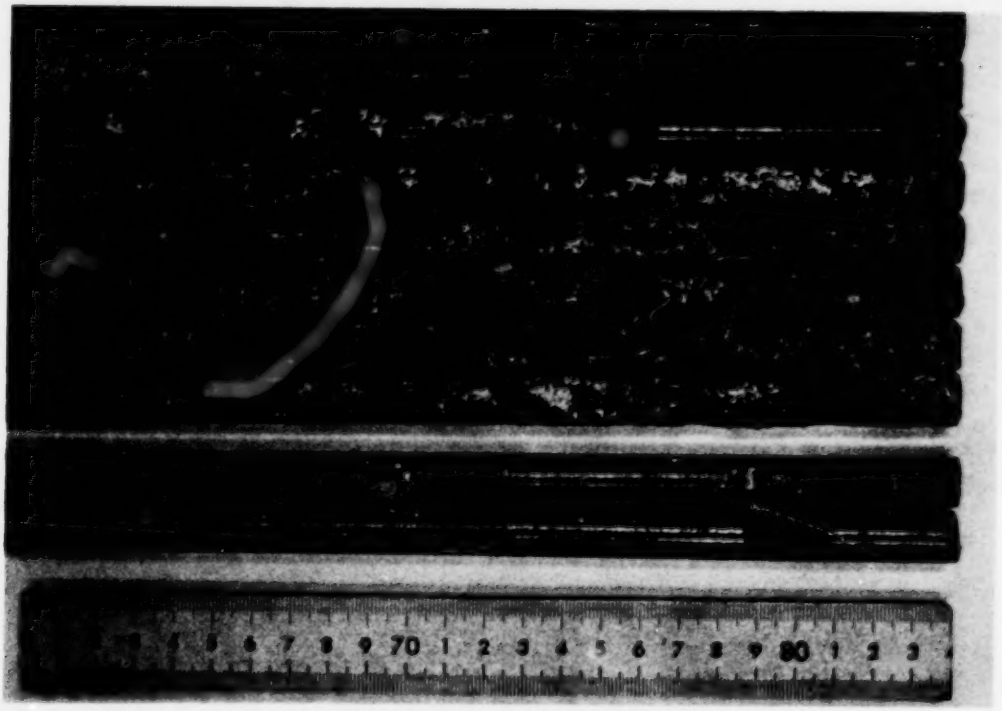

Figure 13/ Corrosion on the Steel Embedded in the Microcell Slabs Subjected to the Oven-Dried Cycle

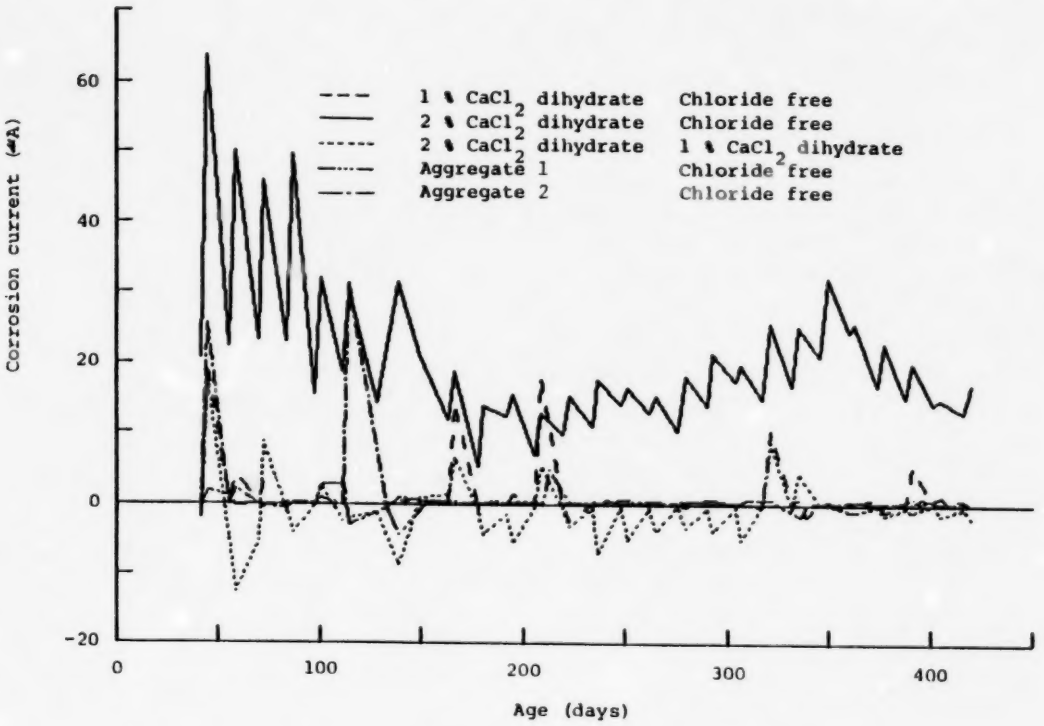

Figure 14/ Corrosion Currents in the Indoor Macrocell Slabs

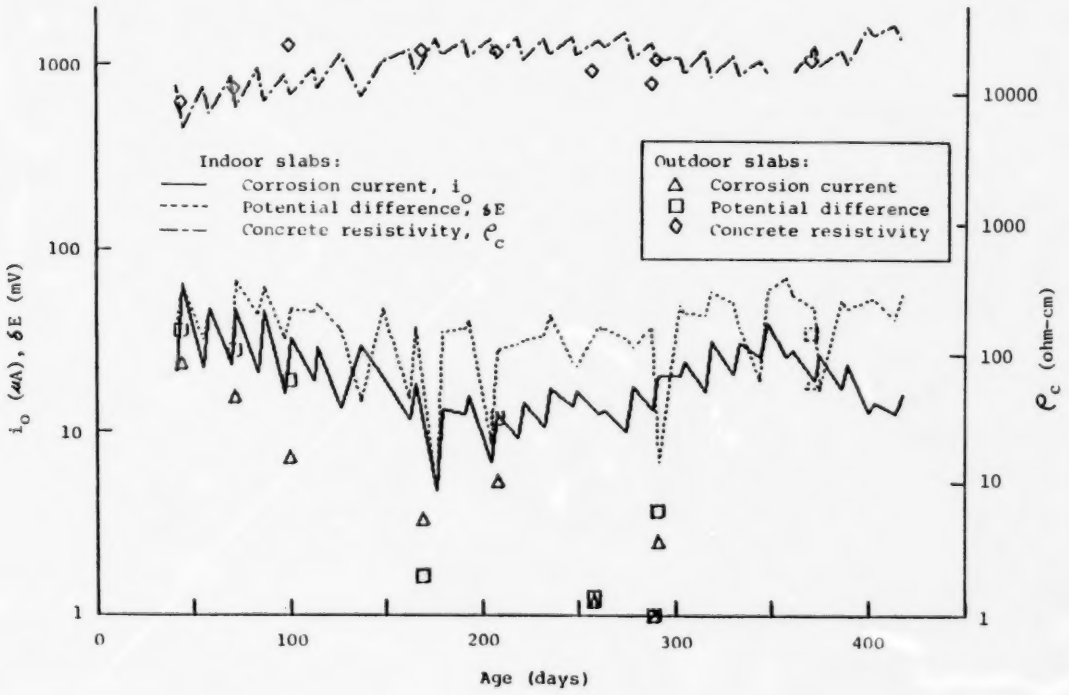

Figure 15/ Corrosion Currents, Anode/Cathode Potential Differences and Concrete Resistivities for the 2% Chloride to Chloride-Free Macrocell Slabs

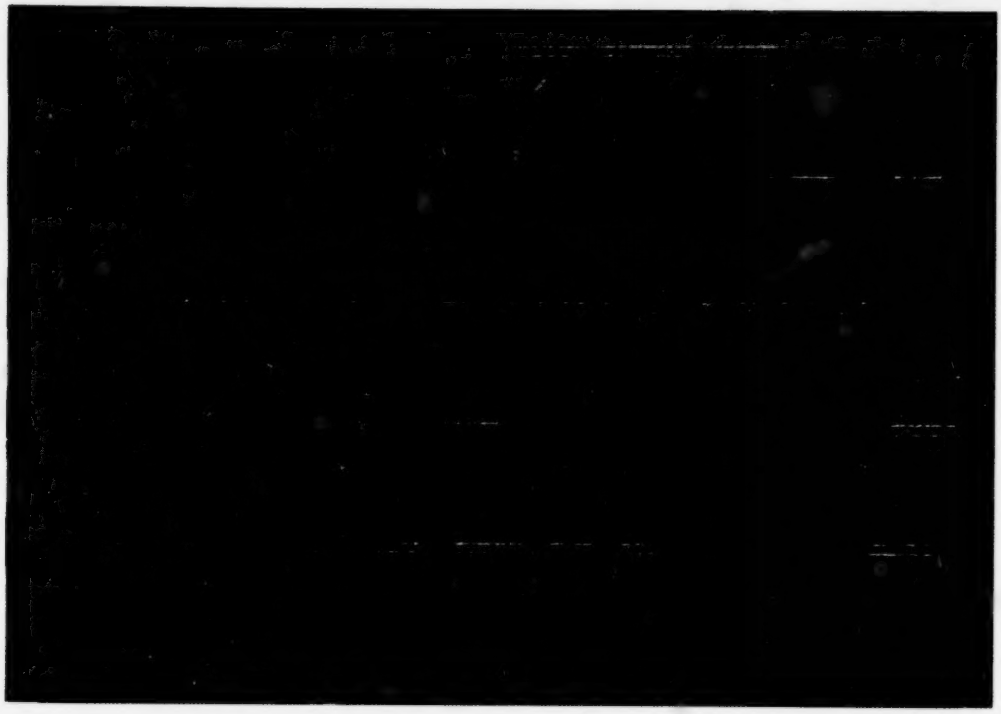

Figure 16/ Corrosion on the Anode Steel Embedded in the Outdoor Macrocell Slabs

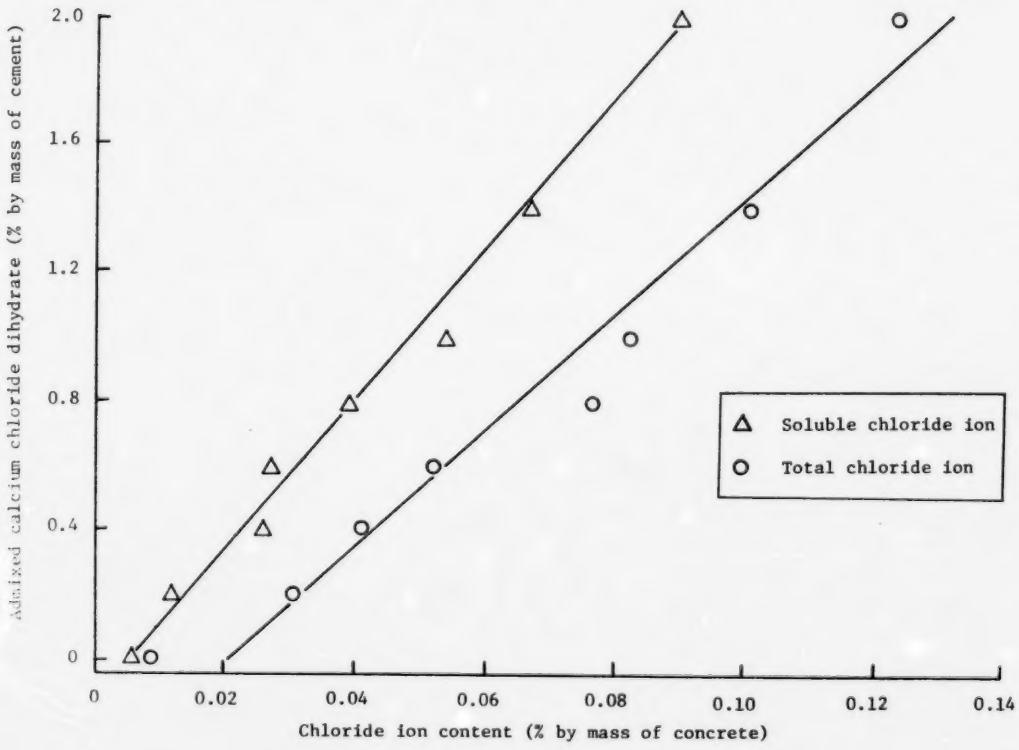

Figure 17/ Measured Chloride Contents of the Admixed Chloride Concrete